Substrate Integrated Waveguide Slot Array Antenna for 77 GHz Automotive Angular Radar Applications

**Xin Liao, Xing Jiang*, Xue-Long Zhu, Lin Peng, Kai-Fa Wang,
Ji-Heng Wang, and Li-Mei Huang**

Abstract—A single-layer substrate integrated waveguide (SIW) longitudinal slot array antenna with low sidelobe level (SLL) in H plane and wide beamwidth in E plane is presented for 77 GHz millimeter-wave angular radar applications. The radiation energy of the antenna is determined by the length and offset of the slot. The conductance of the slot that satisfies the Taylor distribution can effectively suppress the sidelobe of antennas. Measured results indicate that the SLL of the E plane is -28.5 dB, and the 3 dB beamwidth is $98.3°$. A measured peak gain of 12.7 dB is observed with a -10 dB impedance bandwidth of 75.5 GHz $\sim$ 77.4 GHz. The measured results are in good agreement with the theoretical calculations, and the proposed antenna has been demonstrated as a promising candidate used for millimeter-wave automotive angular radar for the proposed antenna array.

1. INTRODUCTION

Millimeter-wave (mmw) radar has attracted growing attention in a wide range of applications [1]. High gain and narrow FOV (the field of view) features permit the implementation of long-range detectors, which may be used in long-range radar (LRR). However, a relatively lower gain and wider FOV are used in medium-range radar (MRR) and short-range radar (SRR) [2]. The automotive angular radar with an MRR or SRR is extensively used in application scenarios such as blind-spot monitoring (BSD), side lane collision warning, and lane change assistance (LCA). The sufficiently large antenna FOV such as the sector-wide beam is very effective to detect the targets in a wide range.

The antenna system is one of the main differentiating factors of a radar sensor, which has attracted a considerable amount of interest from both industry and academia [3]. At present, the microstrip antenna is widely used in vehicle anti-collision radar antenna systems because it is easy to fabricate and integrate with microwave circuits. However, there are also many disadvantages in the microstrip antenna at the same time such as radiation loss, dielectric loss, electromagnetic scattering, and the performance of SLL. The substrate integrated waveguide (SIW) intensively investigated in [4] has become an attractive technology for mmw-antenna arrays. As shown in [5, 6], SIW has many advantages, such as high Q value, low radiation loss, ease of manufacture, and easy integration with other components. Besides, owing to the cavity structure of SIW, a better anti-interference between the antenna array and mmw monolithic microwave integrated circuit (MMIC) can be achieved. The spacing between adjacent SIW slots is a half wavelength, while the spacing between adjacent patches for microstrip antenna is one wavelength, thus, more radiation elements can be placed in the same area.

Low sidelobe antenna arrays play a critical role in improving automotive radar performance [7, 8]. As a strong interference would be caused by high SLLs to the reception signal of the main lobe,

suppressing the SLL of the antenna array can effectively improve the reliability of the automotive radar system.

In this paper, a single-layer wide beamwidth, low SLL SIW slot array antenna satisfying the requirements of the angular radar application at 77 GHz band is proposed and demonstrated. The array of this antenna consists of 14 longitudinal slot elements that satisfy Taylor distribution. To get different weighting values for each slot, the slot's parameter extraction model was used to obtain the slot's parameters, and the radiation energy of the slot can be controlled by tuning the slot length and offset.

1.1. Antenna Configuration

The configuration of the proposed SIW slot array antenna can be found in Figure 1, whose overall size is 47 mm × 15 mm (includes flange). There are 1 × 14 slots in total on the broad wall of the SIW, and the feed mode of the antenna in a rectangular waveguide converts to SIW. All the structures are designed on a dielectric substrate Rogers5880 ($\varepsilon_r = 2.2$ @10 GHz, thickness $h = 0.254$ mm), and the metal used in the substrate is copper with a thickness of 17 µm. Considering the antenna performance and convenience of testing, FR4 substrate material with thickness of 1 mm and dielectric constant of 4.4 was selected to strengthen the structure. For the bonding of antenna and substrate, the thickness of 0.127 mm and dielectric constant of 4.4 of FR4 solidified sheet were selected.
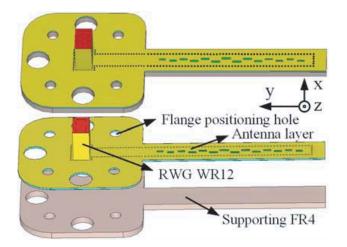

Figure 1. The geometry of the proposed array antenna.

The configuration parameter of the SIW antenna array is shown in Figure 2. The thickness and width of the SIW are h and a_{siw}, respectively. The metallic post separated by a distance s is placed periodically with diameter d. To ensure that the resonant frequency, transmission loss, and transmission mode achieve the design requirements, an accurate analysis is important for a SIW structure size. The
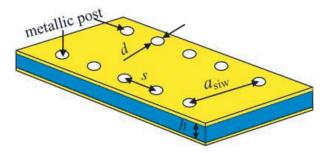

Figure 2. Configuration of the proposed SIW transmission line.

SIW is equivalent to a conventional rectangular waveguide filled with dielectric [9, 10].

$$a_{siw} = \frac{a_{rwg}}{\xi_1 + \cfrac{\xi_2}{\cfrac{s}{d} + \cfrac{\xi_1 + \xi_2 - \xi_3}{\xi_3 - \xi_1}}} \tag{1}$$

a_{rwg} is the width of the equivalent waveguide, where

$$\xi_1 = 1.0198 + \frac{0.3465}{\dfrac{a_{siw}}{s} - 1.0684} \tag{2}$$

$$\xi_2 = -0.1183 - \frac{1.2729}{\dfrac{a_{siw}}{s} - 1.201} \tag{3}$$

$$\xi_3 = 1.0082 - \frac{0.9163}{\dfrac{a_{siw}}{s} + 0.2152} \tag{4}$$

Then, consider the realizability of SIW metallic post-machining and the smaller smaller loss of transmission line. According to the experimental formula [11], the diameter (d) and adjacent spacing (s) of the metallic post should satisfy the following inequality.
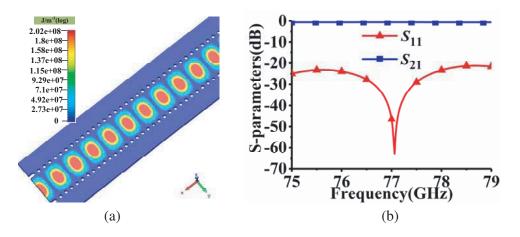
$$d < s < 2d \tag{5}$$

As the ratio (s/d) of the adjacent spacing and the diameter of metallic posts increases, the leakage loss will be reduced. Some detailed data of the SIW transmission line are listed in Table 1.

Table 1. Size of SIW transmission line (unit: mm).

a_{siw}	s	d	h
2.4	0.4	0.25	0.254

The field distribution diagram under the main mode transmission is provided in Figure 3(a) which shows rare electromagnetic leakage. The simulated S-parameters curves are shown in Figure 3(b). The loss of the transmission line is about -1.6 dB, and return loss is greater than 20 dB from 75 GHz to 79 GHz.

(a)   (b)

Figure 3. Simulation results of the SIW transmission line. (a) Electronic model distribution. (b) S-parameter.

1.2. Slots Parameter Extraction

Standard Elliott's design procedure [12–15] is mature and widely used for the design of resonant waveguide slot arrays. The scattering property of a single slot is required in this procedure which is a function of slot length and offset. Stevenson proposed the relationship between slot resonant conductance and offset [20].

$$g \approx 2.09 \frac{a_{rwg}}{h} \frac{\lambda_g}{\lambda} \cos^2(\frac{\pi\lambda}{2\lambda_g}) \sin^2(\frac{\pi x_n}{a_{rwg}}) \tag{6}$$

The relationship between slot conductance and offset x_n is provided in Equation (3).

The low sidelobe performance of antenna element is designed by Taylor synthesis method. The SLL performance of -35 dB is achieved by the array composed of 14 cells, and the current distribution of each unit is shown in Table 2.

Table 2. Normalized excitation amplitude distribution of each unit.

unit	current	unit	current	unit	current
1	0.2975	6	0.9304	11	0.6488
2	0.3671	7	1.000	12	0.4925
3	0.4925	8	1.000	13	0.3671
4	0.6488	9	0.9304	14	0.2975
5	0.8051	10	0.8051		

Slots parameter extraction is one of the methods to obtain the relationship function of conductance, offset, and resonance length [16, 17]. In [16–18], the relationship between the admittance characteristics and resonance length, and the offset of the slot are studied. By this method, the corresponding length and offset of the slot cell can be determined, which is in different power distribution ratios under resonance conditions. The slot parameter extraction model is shown in Figure 4.
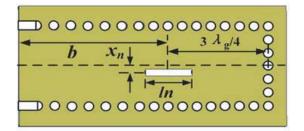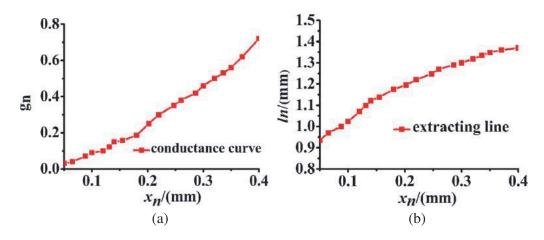

Figure 4. Parameter extraction model of the single radiant slot.

To locate the slots at the peak of the standing wave, the distance between the short circuit and the center of the slot is 3 quarter-wavelengths (can be any odd times of quarter-wavelength). According to the transmission line theory, the admittance y at the slot center is:

$$y = \frac{y_o + j \tan(\beta 3\lambda_g/4)}{1 + jy_o \tan(\beta 3\lambda_g/4)} \tag{7}$$

where y_0 is the normalized admittance of load. β is an integer multiple of the waveguide wavelength. Therefore, the admittance at the port is equal to the center slot, and the admittance at the port can be used as the admittance of the isolated slot.

$$y_n = \frac{1 - |S_{11}|}{1 + |S_{11}|} \tag{8}$$

(a) (b)

Figure 5. Extraction results of slot parameters. (a) The relationship between offset and normalized conductance. (b) The relationship between slot length and offset.

By repeatedly adjusting the length and offset of the slot, the slot is in a resonance state when port S_{11} resonates at 77 GHz, and the imaginary part of admittance is zero. As shown in Figures 5(a) and (b), the relationship among the offset of the gap, the conductance, and the resonant length is given below.

The longitudinal slots on the top metallic plate are placed alternately on both sides of the centerline to perturb the surface current for radiation. Adjacent radiating slots are staggered and placed 180 degrees out of phase on both sides of the centerline. Therefore, the spacing (d) with half of the waveguide wavelength is designed in order to stimulate all slot elements in the same phase, and the distance (e_s) between the terminal slot and the short-circuited wall is three-quarters of the waveguide wavelength at the design frequency. The antenna configuration is shown in Figure 6.
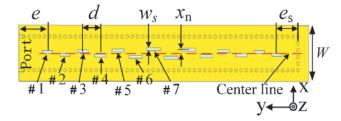

Figure 6. Configuration of the SIW slot array.

The resonant length and offset of slots (♯ 1, ♯ 2, ♯ 3, ♯ 4, ♯ 5, ♯ 6, ♯ 7) are listed in Table 3.

Table 3. The resonant length and offset of slot (unit: mm).

ele	l_n	x_n	ele	l_n	x_n
♯ 1	1.023	0.102	♯ 1	1.318	0.321
♯ 2	1.041	0.121	♯ 2	1.248	0.247
♯ 3	1.088	0.127	♯ 3	1.166	0.202
♯ 4	1.152	0.145	♯ 4	1.152	0.145
♯ 5	1.166	0.202	♯ 5	1.088	0.127
♯ 6	1.248	0.247	♯ 6	1.041	0.121
♯ 7	1.318	0.321	♯ 7	1.023	0.102

The extraction results can be served as initial values for the further accurate optimization by the full-wave simulations of the linear SIW array, thus the efficiency of the designed antenna could be improved by this process.

1.3. Waveguide-to-SIW Transition

The traditional microstrip feed has a large loss in the high-frequency band of 79 GHz, so it is necessary to design a waveguide to SIW structure for processing and testing antenna [4, 16]. There is a pressing need for an effective transition between air-filled rectangular waveguide (RWG) and SIW. A WR-12 waveguide to SIW vertical transition is designed in Figure 7.
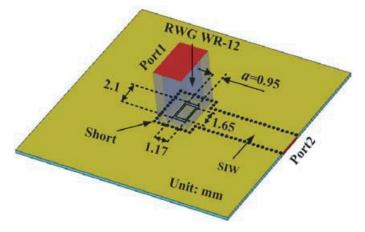

Figure 7. Configuration of the transition.

As shown in Figure 7, an annular slot window is etched on the broad wall of SIW (the top surface of SIW), and the incident wave in SIW radiates into the RWG through the slot. A short circuit is placed at the end of the SIW line, to obtain the reflection energy superimposed with the same phase, and the distance between the short circuit and the center of the patch is three quarter-wavelengths.

The upper layer patch plays a role of impedance transformation and mode conversion. The equivalent circuit of the transition structure is shown in Figure 8. The long side of the annular slot is equivalent to capacitors C1 and C2, respectively, and the width and position of the slot affect the capacitance. Besides, the equivalent capacitance between the patch and the floor is C3 which varies with the size and position of the patch. The short circuit metal column is equivalent to inductance L_S.
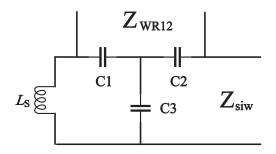

Figure 8. Equivalent circuit of the transition structure.

Figure 9(a) shows the effect of the upper reflector width on the impedance bandwidth of the antenna. The resonance point is negatively correlated with the value of a. When $a = 0.93$, 0.95, and 0.97 mm, the corresponding resonance points are 77.8, 77, and 76 GHz, respectively. From Figure 9(b), the return loss of the transition bandwidth from 73 GHz to 80 GHz is better than 10 dB, and the insertion loss is less
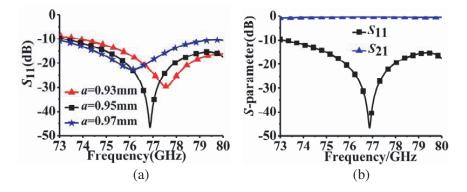
Figure 9. Simulation results of the transition. (a) The effect of patch width on S parameter. (b) S-parameter.

than 0.8 dB over the frequency range of 73–80 GHz. The proposed transition structure provided with wide bandwidth, low insertion loss, and designed on one layer with a simple structure is demonstrated, and these advantages make it acceptable for use.

1.4. Design of Radiating Array

The parameters of the slot are obtained by the parameter extraction model, which provides a design reference and reduces the design cycle to a great extent. However, the mutual coupling effect between slots is not considered in the isolated slot parameter extraction model. There is also tolerance in the extracted slot parameters. The slot parameters extracted by electromagnetic simulation software are only the basis of the preliminary linear matrix model construction which is need to be further optimized. Usually, some tunings of the slot offset and/or length may achieve the desirable results (SLL below -35 dB in the H-plane).
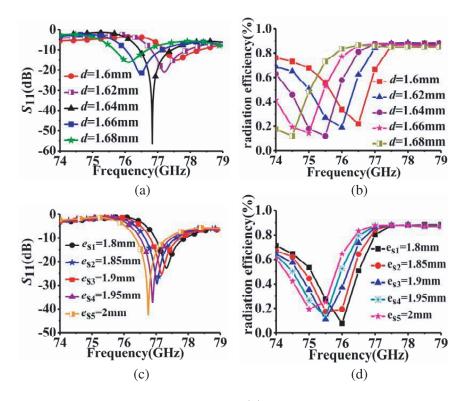
All radiating elements have the same phase, and their amplitude distributions must be arranged carefully to achieve the given gain and low side-lobe level. Simulated S-parameters and radiation efficiency are presented in Figure 10. We can notice that the results are changed regularly by tuning the spacing of adjacent slots and the distance of slots from the terminal on matching.

From Figure 10, it can be seen that the port impedance matching and radiation efficiency are optimal when the slot distance $d = 1.64$ mm and the slot distance from the terminal $e_s = 1.95$ mm. The operational frequency band of the antenna is 76.5 GHz–77.5 GHz, whose resonant point is 76.8 GHz, and the radiation efficiency reaches 82%.

From Figure 11, it can be seen that the current is very strong in the slots, while being weak in the other areas on the upper metal layer. It should be noted that the longitudinal current vector of each slot is symmetrically distributed, which leads to current counterbalance. Then, the simulated radiation patterns of the SIW slot antenna at different W of 77 GHz are shown in Figure 12. The results are shown in Table 4. When $W = 4.1$ mm, 4.2 mm, 4.3 mm, and 4.4 mm, the corresponding 3 dB beamwidth is 83°, 89°, 94°, 106°, and the 6 dB beamwidth is 124°, 141°, 148°, and 156°, respectively. The corresponding gains are 13.7 dB, 13.6 dB, 13.4 dB, and 12.8 dB. The simulated HPBW of 15° in the H-plane is more

Table 4. The corresponding beam width of different W.

W (mm)	4.1	4.2	4.3	4.4
E-plane HPBW	83°	89°	94°	106°
E-plane 6 dB BW	124°	141°	148°	156°
H-plane HPBW	15°	15°	15°	15°
Gain (dBi)	13.7	13.6	13.2	12.8

Figure 10. Simulation results of radiating array. (a) The effect of the spacing d on S_{11}. (b) The effect of the spacing d on radiation efficiency. (c) The effect of parameter e_s on S_{11}. (d) The effect of parameter e_s on radiation efficiency.
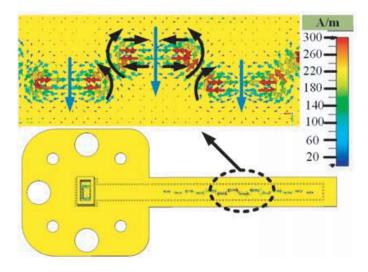

Figure 11. The diagram of slots current.

stable than the E-plane over 4.1–4.4 mm. For the slot antenna on the infinite ground, the plane can be equivalent to a magnetic dipole antenna when the slot width is much less than the wavelength. The radiation pattern of the antenna in the E-plane is omnidirectional when the metal ground is infinite [19]. Scattering is generated at the edge of the metal ground. Therefore, the radiated magnetic currents and mirroring magnetic currents cannot be superposed together at the end-fire angle. However, the wide beamwidth radiation performance of the antenna is not affected.
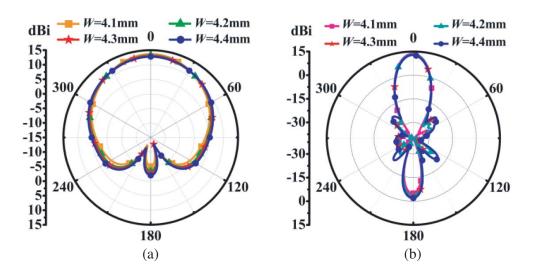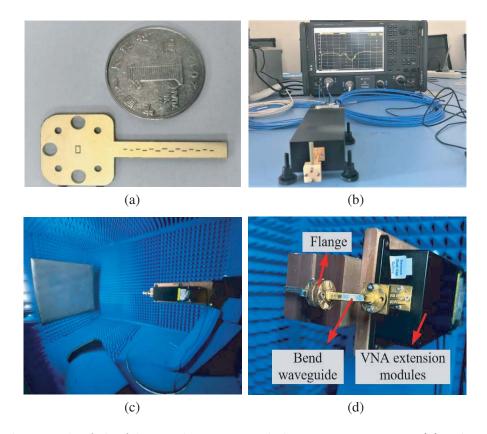
Figure 12. Radiation patterns of the SIW-slot antenna of different W. (a) E-plane. (b) H-plane.

Figure 13. Photograph of the fabricated antenna and the test environment. (a) Fabricated antenna. (b) Standing wave test environment. (c) Tightening field test. (d) Detail of the antenna mount.

2. EXPERIMENTAL VALIDATION AND DISCUSSION

According to the above discussions, the proposed single layer wide beam array antenna was fabricated and measured. The antenna processing object is shown in Figure 13(a). The array antenna is conveniently surface-mounted to the standard flange of the waveguide by creating a flange hole on
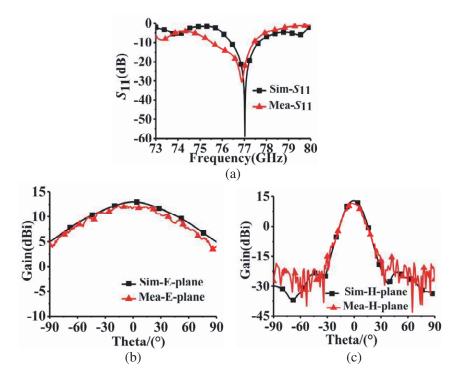
Figure 14. Simulated and measured. (a) S_{11} of the array antenna. (b) (c) Radiation pattern of the array antenna at 77 GHz.

the substrate. The test environment is shown in Figures 13(b) and (c). All of the measurement setups are controlled by the CATR (compact antenna test range) test system (the maximum angle test range of the system is $(-90°, 90°)$. Figure 13(d) shows the adapter required for the test, including the bend waveguide and flange.

The simulated and measured reflection coefficients of the proposed array antenna are shown in Figure 14(a). The measured results are consistent with the simulation ones. The simulated bandwidth less than -10 dB is in 76.3–77.6 GHz, and the measurement is from 75.5 to 77.4 GHz.

The comparison between the actual measurement and simulation of the pattern is shown in Figures 14(b) and (c), and a good agreement was achieved between the simulated and measured radiation patterns. The simulated 3 dB and 6 dB beamwidths in the E-plane (xoz plane) are about 93.6° and 147.2°, respectively, while the HPBW in the H-plane (yoz plane) was approximately 15.9°. The measured 3 dB and 6 dB beamwidths in the E-plane are about 98.3° and 148.4°, respectively, while the HPBW in the H-plane was approximately 15.4°. The simulated and measured sidelobe levels in the H-plane are below -35 dB and -28 dB, respectively. The simulated and measured peak gains are 13.2 dBi and 12.2 dBi, respectively. Due to the introduction of bent waveguide and flange, the gain-loss is about 1 dB.

3. CONCLUSION

A single-layer substrate integrated waveguide (SIW) longitudinal slot array antenna with low sidelobe level (SLL) in the H-plane and wide beamwidth in the E-plane is presented for 77 GHz millimeter-wave angular radar applications. The slot parameters are obtained by using the slot parameter extraction model, and the linear array of 14 elements adopts Taylor distribution. The offset and harmonic length of each slot are used to obtain excitation and control the low sidelobe level. The test results show that the gain of the proposed antenna is 12.2 dB, and 3 dB and 6 dB beamwidths in the E-plane are about 98.3° and 148.4°, respectively. Low SLL less than -28 dB and stable boresight radiation are achieved. Therefore, the proposed SIW slot array antenna is validated to be a valuable candidate for high performance automotive angular radar applications.

ACKNOWLEDGMENT

REFERENCES

1. Hasch, J., E. Topak, R. Schnabel, et al., "Millimeter-wave technology for automotive radar sensors in the 77 GHz frequency band," *IEEE Transactions on Microwave Theory and Techniques*, Vol. 60, No. 3, 845–860, 2012.

2. Menzel, W. and A. Moebius, "Antenna concepts for millimeter-wave automotive radar sensors," *Proceedings of the IEEE*, Vol. 100, No. 7, 2372–2379, 2012.

3. Hirokawa, J. and M. Ando, "Single-layer feed waveguide consisting of posts for plane TEM wave excitation in parallel plates," *IEEE Transactions on Antennas and Propagation*, Vol. 46, No. 5, 625–630, 1998.

4. Martinez-Ros, A. J., J. L. Gómez-Tornero, and G. Goussetis, "Holographic pattern synthesis with modulated substrate integrated waveguide line-source leaky-wave antennas," *IEEE Transactions on Antennas and Propagation*, Vol. 61, No. 7, 3466–3474, 2013.

5. Yang, H., G. Montisci, Z. Jin, et al., "Improved design of low sidelobe substrate integrated waveguide longitudinal slot array," *IEEE Antennas and Wireless Propagation Letters*, Vol. 14, 237–240, 2014.

6. Huang, G. L., S. G. Zhou, T. H. Chio, et al., "A low profile and low sidelobe wideband slot antenna array feb by an amplitude-tapering waveguide feed-network," *IEEE Transactions on Antennas and Propagation*, Vol. 63, No. 1, 419–423, 2014.

7. Cheng, Y. J., H. Xu, D. Ma, et al., "Millimeter-wave shaped-beam substrate integrated conformal array antenna," *IEEE Transactions on Antennas and Propagation*, Vol. 61, No. 9, 4558–4566, 2013.

8. Cai, Y., Z. Qian, Y. Zhang, et al., "A compact wideband SIW-fed dielectric antenna with end-fire radiation pattern," *IEEE Transactions on Antennas and Propagation*, Vol. 64, No. 4, 1502–1507, 2016.

9. Xu, F. and K. Wu, "Guided-wave and leakage characteristics of substrate integrated waveguide," *IEEE Transactions on Microwave Theory and Techniques*, Vol. 53, No. 1, 66–73, 2005.

10. Cassivi, Y., L. Perregrini, P. Arcioni, et al., "Dispersion characteristics of substrate integrated rectangular waveguide," *IEEE Microwave and Wireless Components Letters*, Vol. 12, No. 9, 333–335, 2002.

11. Yan, L., W. Hong, K. Wu, et al., "Investigations on the propagation characteristics of the substrate integrated waveguide based on the method of lines," *IEE Proceedings — Microwaves, Antennas and Propagation*, Vol. 152, No. 1, 35–42, 2005.

12. Guo, Q. Y. and H. Wong, "Wideband and high-gain Fabry-Pérot cavity antenna with switched beams for millimeter-wave applications," *IEEE Transactions on Antennas and Propagation*, Vol. 67, No. 7, 4339–4347, 2019.

13. Elliott, R., "An improved design procedure for small arrays of shunt slots," *IEEE Transactions on Antennas and Propagation*, Vol. 31, No. 1, 48–53, 1983.

14. Elliott, R. and W. O'Loughlin, "The design of slot arrays including internal mutual coupling," *IEEE Transactions on Antennas and Propagation*, Vol. 34, No. 9, 1149–1154, 1986.

15. Elliott, R. and L. Kurtz, "The design of small slot arrays," *IEEE Transactions on Antennas and Propagation*, Vol. 26, No. 2, 214–219, 1978.

16. Stern, G. and R. S. Elliott, "Resonant length of longitudinal slots and validity of circuit representation: Theory and experiment," *IEEE Transactions on Antennas and Propagation*, Vol. 33, No. 11, 1264–1271, 1985.

17. Stevenson, A. F., "Theory of slots in rectangular waveguides," *Journal of Applied Physics*, Vol. 19, No. 1, 24–38, 1948.

18. Lu, H. C. and T. H. Chu, "Equivalent circuit of radiating longitudinal slots in substrate integrated waveguide," *IEEE Antennas and Propagation Society Symposium, 2004*, Vol. 3, 2341–2344, IEEE, 2004.

19. Wen, Y. Q., B. Z. Wang, and X. Ding, "Wide-beam SIW-slot antenna for wide-angle scanning phased array," *IEEE Antennas and Wireless Propagation Letters*, Vol. 15, 1638–1641, 2016.

20. Stevenson, A. F., "Theory of slots in rectangular wave-guides," *Journal of Applied Physics*, Vol. 19, No. 1, 24, 1948.